Highly anisotropic and two-fold symmetric superconducting gap in nematically ordered FeSe_{0.93}S_{0.07}

H. C. Xu,¹ X. H. Niu,¹ D. F. Xu,¹ J. Jiang,¹ Q. Yao,¹ M. Abdel-Hafiez,^{2,3} D. A. Chareev,⁴ A. N. Vasiliev,⁵ R. Peng,^{1,*} and D. L. Feng^{1,†}

¹State Key Laboratory of Surface Physics, Department of Physics, and Advanced Materials Laboratory, Fudan University, Shanghai 200433, People's Republic of China ²Center for High Pressure Science and Technology Advanced Research, Shanghai 201203, China ³Faculty of science, Physics department, Fayoum University, 63514-Fayoum, Egypt ⁴Institute of Experimental Mineralogy, Russian Academy of Sciences, 142432 Chernogolovka, Moscow District, Russia ⁵Low Temperature Physics and Superconductivity Department, M.V. Lomonosov Moscow State University, 119991 Moscow, Russia (Dated: October 2, 2018)

FeSe exhibits a novel ground state in which superconductivity coexists with a nematic order in the absence of any long-range magnetic order. Here we report an angle-resolved photoemission study on the superconducting gap structure in the nematic state of FeSe_{0.93}S_{0.07}, without the complication caused by Fermi surface reconstruction induced by magnetic order. We found that the superconducting gap shows a pronounced 2-fold anisotropy around the elliptical hole pocket near the Z point of the Brillouin zone, with gap minima at the endpoints of its major axis, while no detectable gap was observed around the zone center and zone corner. The large anisotropy and nodal gap distribution demonstrate the substantial effects of the nematicity on the superconductivity, and thus put strong constraints on the current theories.

PACS numbers: 74.70.Xa, 74.25.Jb, 74.20.Mn

The pairing mechanism underlying unconventional superconductivity is often related to the quantum fluctuations of nearby orders. In most Fe-based superconductors, both magnetic and nematic orders appear simultaneously near the superconducting state. Accordingly, both spin-fluctuationmediated and orbital-fluctuation-mediated superconducting pairing mechanisms have been proposed [1–5]. Although intense experimental studies have been conducted [6–13], the exact pairing mechanism of Fe-based superconductors is still under heated debate.

FeSe is a unique material with a novel superconducting state. Orbital order develops in the nematic state of FeSe without breaking the translational symmetry as shown by angle resolved photoemission spectroscopy (ARPES) studies [14, 15]. The superconductivity coexists with the nematic order without any long range magnetic order [16], thus disentangling the magnetic and orbital orders. Moreover, recent results suggest that FeSe is a quantum paramagnet [4] with coexisting Néel and stripe antiferromagnetic interactions [17, 18]. The novel ground state in FeSe provides a fresh perspective for studying the effect of nematic order on the superconducting gap structure in the absence of the Fermi surface reconstruction induced by magnetic order, which helps to reveal the roles of spin and orbital degrees of freedom in unconventional superconductivity. A nodeless superconducting gap structure in FeSe was suggested by previous reports on specific heat [19], Andreev reflection spectroscopy [20], and thermal conductivity measurements [21]. In contrast, scanning tunnelling spectroscopy (STS) studies on FeSe films [22] and transport measurements on bulk $FeSe/FeSe_{1-x}S_x$ crystals with improved quality [23, 24] all demonstrate a nodal gap structure. However, due to the low T_c and small gap size of FeSe/FeSe_{1-x}S_x single crystals, the gap distribution in momentum-space is still unknown.

In this work, we studied the superconducting gap structure of high-quality $FeSe_{0.93}S_{0.07}$ single crystals ($T_c=10~\rm K$) with high resolution ARPES [25]. At 6.3 K, both the nematic electronic structure and the superconducting gap are observed. The gap amplitude at the hole pocket is 2.5 meV, similar to that measured by STS [23]. The superconducting gap shows 2-fold anisotropy around the Z point, and is undetectable around the hole Fermi surface near the zone center and the electron pockets at the zone corners. We find that the unique gap structure observed here cannot be resonably fitted by most known theoretical gap structures and their simple combinations, which suggest that the effects of nematicity on the superconductivity are substantial.

FeSe $_{0.93}$ S $_{0.07}$ single crystals were grown using AlCl $_3$ /KCl flux in a temperature gradient (from 400 °C to ~50 °C) for 45 days [25, 26]. The ARPES measurements were conducted at the I05 beamline at the Diamond Light Source. The data were taken at the temperature of 6.3 K unless otherwise specified. The single crystals were cleaved in-situ and measured under ultra-high vacuum of 1×10^{-10} mbar. For data collection with 23 eV (37 eV) photons, the energy resolution was 3 meV (5 meV). Empirically, this allows resolving a superconducting gap of 0.6 meV (1 meV).

Figure 1(a) illustrates the Fermi surfaces of FeSe/FeSe_{1-x}S_x in the nematic state, which consist of one hole pocket at the zone center and one electron pocket at the zone corner of the 2-Fe Brillouin zone [14, 28]. There is another electron pocket (δ) around A₁/A₂ according to the calculation and quantum oscillation measurements[14, 28], but it has not been detected by ARPES probably due to its small matrix element [14]. In our data, the elliptical hole pocket α around the Z point is resolved in Fig. 1(b). Another elliptical hole pocket α' , with weaker spectral intensity, is contributed by 90 °-rotated twin domains. The distribution of spectral weight is nearly iden-

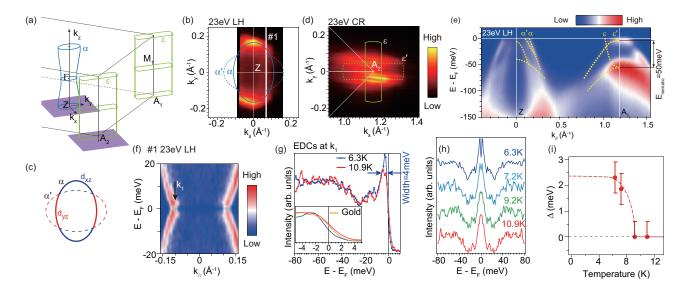


FIG. 1: (color online). (a) Fermi suface topology in the 2-Fe Brillouin zone of FeSe in the nematic state according to Refs. [14]. (b) Fermi surface mapping around the Z point with linear-horizontal (LH) polarized photons. The corresponding momenta are indicated by the purple square in panel (a). (c) Orbital contents of pocket α (solid ellipse) and its counterpart from another twin domain (α' , dashed ellipse) according to ref. [14]. (d) Same as (b) but around the A_2 point with circular-right (CR) polarized photons.(e) Photoemission intensity along Z-A₁. The band splitting $E_{nematic}$ due to nematic orbital ordering is indicated. (f) Symmetrized photoemission intensity along cut #1 as indicated in panel (c). (g) Energy distribution curves (EDCs) above and below T_c at the momentum k_1 in panel (f). The width of the superconducting quasiparticle peak is indicated. The inset shows the leading edge shift near the Fermi energy. (h) Temperature dependent symmetrized EDCs at momentum k_1 . (i) Superconducting gap size as a function of temperature fits to the Bardeen-Cooper-Schrieffer formula.

tical to that of FeSe under the same experimental geometry with linear horizontal polarized photons [14], indicating the similar orbital contents on the α pocket [Fig. 1(c)]. The electron pocket ε around the zone corner (A₁/A₂) is elongated [Fig. 1(d)]. Figure 1(e) shows the photoemission spectra along Z-A₁, clearly indicating the splitting of 50 meV between bands ε and ε' due to the nematic order [14].

At 6.3 K, band α shows a back-bending dispersion and gap opening [Fig. 1(f)], which are the hallmarks of Bogliubov quasiparticles. Sharp quasiparticle peaks are observed at the Fermi crossings of band α at 10.9 K, and become even sharper at 6.3 K [Fig. 1(g)], indicating the high quality of the FeSe_{0.93}S_{0.07} single crystals. From 10.9 K to 6.3 K, the leading edge shifts below the Fermi energy [inset of Fig. 1(g)], indicating the opening of the superconducting gap. The superconducting gap size determined by the symmetrized energy distribution curves (EDCs) is around 2.5 meV at 6.3K [Fig. 1(h)], which decreases with increasing temperature and eventually closes around 9.2 K following the Bardeen-Cooper-Schrieffer formula [Fig. 1(i)], consistent with the T_c of 10 K measured by transport experiments [25].

The momentum distribution of the superconducting gap on the hole pockets α and α' has been studied along the parallel momentum cuts in Fig. 2(a) with 23 eV photons. In the symmetrized photoemission intensity along cut #2, α' is gapped at momenta k_3 and k_4 , whereas α crosses the Fermi level at momenta k_2 and k_5 without any observable gap opening [Fig. 2(b)], indicating distinct gap sizes between the momenta near the major axis endpoints of pocket α and those

near the minor axis endpoints of pocket α' . As shown by the symmetrized EDCs in Fig. 2(c), the superconducting gap is reduced around the major axis endpoints of the elliptical Fermi surface α ($\theta \simeq 90$ ° and 270°). Around the minor axis endpoints of pocket α' , the gap size remains constant [Fig. 2(d)]. By the empirical fitting to a superconducting spectral function [30], the sizes of superconducting gap as a function of polar angle θ are summarized in one single polar plot [Fig. 2(e)], noting that the α and α' are identical bands from twin domains. The superconducting gap on band α shows anisotropy with 2-fold symmetry. The gap size decreases from about 2.5 meV at the minor axis endpoints of the ellipse, to less than 0.6 meV around the major axis endpoints, which is at the experimental resolution limit.

The photoemission spectra at the Fermi crossing of band ε ' show sharp quasiparticle peaks in the superconducting state [Fig. 2(f)]. However, no superconducting gap is detected along the electron pockets ε or ε ' [Fig. 2(g)]. The absence of a superconducting gap at these momenta indicates nodes or a small gap size below the experimental resolution limit.

Figure 3(a) illustrates the photoemission cuts through bands α and α' around the Γ point with 37 eV photons. The bands α and α' are resolved along cut #3 [Fig. 3(b)], showing sharp quasiparticle peaks at the Fermi crossings [Fig. 3(c)]. Along the elliptical Fermi surface α' , the symmetrized EDCs show no detectable superconducting gap [Fig. 3(d)], indicating nodes or a small gap size below the experimental resolution limit. For band α , the Fermi crossings with polar angles 264.0 ° and 275.0 ° show no observable gap either [Fig. 3(e)].

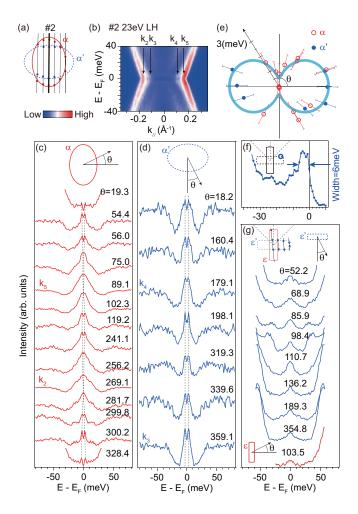


FIG. 2: (color online). (a) Illustration of hole pockets α and α' around the Z point. (b) Symmetrized photoemission intensity along the cut #2 as indicated in panel (a). (c) Symmetrized EDCs on the pocket α . The insets define the in-plane angle θ . (d) Symmetrized EDCs on the pocket α' . (e) Polar plot of the superconducting gap as a function of θ along the pockets α and α' . (f) EDC at the pocket ε' indicated by the blue circle. (g) Symmetrized EDCs on the electron pockets ε and ε around the A_1 point. The pockets ε' and ε are from different twin domains.

The quasiparticle peaks at $\sim \pm 4$ meV for $\theta = 80.6^{\circ}$ and 95.0° are contributed by band α' , which gives false signatures of gap opening in Fig. 3(e). Actually as shown in Figs. 3(f) and 3(g), the EDCs divided by the resolution-convolved Fermi-Dirac function are flat within 2-3 meV of the Fermi crossings of band α , indicating no detectable gap opening. As shown in the Supplementary Material [29], the gap amplitude decreases from Z to Γ untill it diminishes, which is intriguingly opposite to those observed in BaFe₂(As_{1-x}P_x)₂ and Ba_{1-x}K_xFe₂As₂ [30, 31], where the gap of the α band decreases from Γ to Z.

Our results confine the nodes to the vicinity of the two endpoints on the elliptical α pocket around Z, the α pocket around Γ , and the electron pockets. Considering that the STS spectra on superconducting FeSe_{1-x}S_x [23] show finite but small density of states at the Fermi energy at 0.4 K, the nodes can only

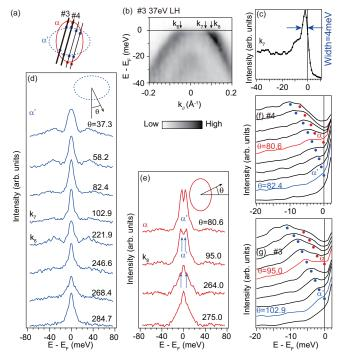


FIG. 3: (color online). (a) Illustration of pockets α and α' around the Γ point. (b) Photoemission intensity along the cut #3 as indicated in panel (a). (c) The EDC at momentum k_7 . (d) Symmetrized EDCs on the pocket α' . The inset defines the in-plane angle θ . (e) Symmetrized EDCs on the pocket α . Quasiparticle peaks from band α' are indicated. (f) EDCs divided by the resolution-convolved Fermi-Dirac function near the upper Fermi crossings of cut #4 in panel (a). (g) Same as panel (f) but near the upper Fermi crossings of cut #3.

occur on a small portion of the Fermi surface, while most of the momenta without a detectable gap in our data must exhibit a finite gap at much lower temperatures. Though the precise positions of nodes in these regions will have to be determined with better resolution in future studies, the momentum dependent gap structure, especially the large gap anisotropy at the α pocket showing remarkable component of $\cos 2\theta$ with 2-fold symmetry [Fig. 4(a)], put constraints on current theories of superconductivity in FeSe. The the observed gap structure can be used to scrutinize four types of current scenarios:

First, in the case of superconductivity with dominant s++ pairing mediated by orbital fluctuations, the gap form is nearly isotropic and nodeless [5]. The large anisotropy and nodal behavior of the gap in FeSe suggest that the superconducting pairing in FeSe is not mediated by pure orbital fluctuations.

Second, in $s\pm$ pairing mediated by magnetic interactions, the sign-changing gap form may lead to gap anisotropy and nodes [32, 33]. Since both Néel and stripe spin-fluctuations exist in FeSe [18], if the $s\pm$ superconducting pairing were generated either by the (π,π) interaction with gap form $\cos k_x \cos k_y$, or by the $(\pi,0)$ interaction with gap form $(\cos k_x + \cos k_y)/2$ [33], the anisotropy of the superconducting gap on the elliptical α pocket would be 3% and 6% for these two gap forms, respectively. These cannot account for

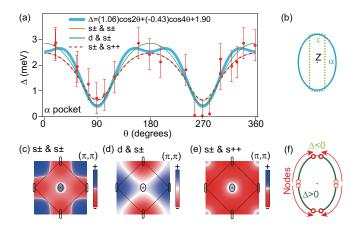


FIG. 4: (color online). (a) Angular dependence of the superconducting gap on the α pocket and fitting results by cosine series, $\Delta_{s\pm,s\pm}$, $\Delta_{d,s\pm}$, and $\Delta_{s\pm,s++}$. (b) Overlapping of the pockets ε (dashed curves) and α (solid curves) in the case of antiferromagnetic folding. (c-e) The gap forms obtained by the fitting results in panel (a). (f) The gap structure on the pocket α according to the theory of Ref. [37].

the large anisotropy of at least 78% observed in our data.

If there were static stripe antiferromagnetic order with wave vector $(\pi, 0)$, the electron pockets would have been folded to the zone center and intersect with the α pocket around the major axis endpoints in FeSe [Fig. 4(b)]. Theory suggests that gap nodes would emerge at the reconstructed Fermi surfaces, given a large value of antiferromagnetic order parameter [34]. However, FeSe shows no static magnetic order, thus its gap anisotropy cannot be explained by this scenario.

Third, a composite form of superconducting pairing may arise from the quantum paramagnet ground state with Néel and stripe spin fluctuations [4, 18]. In Fig. 4(a), we fit the gap anisotropy of the α pocket by [22]

$$\Delta_{s\pm,s\pm} = \Delta_1 \cos k_x \cos k_y + \Delta_2 (\cos k_x + \cos k_y)/2,$$

which gives superconducting gap sizes Δ_1 =-58.2±8.8 meV and Δ_2 =62.2±9.2 meV for $s\pm$ pairing mediated by the two kinds of spin fluctuations. Moreover, the combination of Néel spin fluctuation mediated d-wave pairing and stripe spin fluctuation mediated $s\pm$ pairing with the gap form

$$\Delta_{d,s\pm} = \Delta_d(\cos k_x - \cos k_y)/2 + \Delta_2(\cos k_x + \cos k_y)/2,$$

also gives good fitting with Δ_1 =30.3±2.8 meV and Δ_2 =2.24±0.09 meV [Fig. 4(a)]. Alternatively, by combining the spin-fluctuation-mediated s± pairing and orbital-fluctuation-mediated s++ pairing [5], the gap anisotropy at pocket α can be fitted by

$$\Delta_{s\pm,s++} = \Delta_2(\cos k_x + \cos k_y)/2 + \Delta_s,$$

with Δ_2 =32.8±4.8 meV and Δ_s =-28.7±4.4 meV for $s\pm$ and s++ pairing, respectively [Fig. 4(a)]. All three fittings contain gap amplitudes over 30 meV, which are nonphysical compared with the low T_c of FeSe. Moreover, the obtained gap forms

would give a large gap at the ε pocket [Figs. 4(c)-4(e)], in contrast to the undetectable superconducting gap in our data. Therefore, these simple combinations of gap forms cannot account for the large gap anisotropy on pocket α .

Fourth, we consider an orbital-dependent superconducting pairing symmetry. The orbital anti-phase pairing cannot explain the gap anisotropy on pocket α [35, 36], because the orbital composition changes around $\theta = \pm 45^{\circ}$ and $\pm 135^{\circ}$ [Fig. 1(c)], rather than at the major axis endpoints where the gap minima appear. On the pocket α , the Fermi surface sections showing gap minima and gap maxima coincide with those with d_{xz} and d_{yz} orbital characters, respectively, indicating that the orbital ordering may lead to weaker superconducting pairing of d_{xz} orbital than that of d_{yz} orbital. Alternatively, it was shown that the orbital ordering may mix different pairing symmetries and give rise to pairs of accidental nodes [37]. The positions of the nodes depend on the splitting between d_{xz} and d_{vz} orbital, which was set to 80 meV in the theory, while it is 50 meV in FeSe_{0.93}S_{0.07} [Fig. 1(e)]. In this scenario, if a pair of nodes are located very close to a major-axis endpoint of the α pocket due to a strong nematic order [Fig. 4(f)], the gap would exhibit just one minimum at each endpoint in the data due to the limited momentum resolution, which would be consistent with our findings.

In summary, we have revealed the superconducting gap structure of FeSe_{0.93}S_{0.07} under the effect of nematic order and in the absence of magnetic order for the first time. The remarkable anisotropy of the superconducting gap rules out s++ pairing purely mediated by orbital fluctuations. The gap amplitude decreases from Z to Γ , till it is undetectable at Γ , which is intriguingly different from that of BaFe₂(As_{1-x}P_x)₂ with a nodal ring around Z. A 2-fold anisotropy of the superconducting gap is observed at the α hole pocket around Z, which cannot be understood by current theories unless the effects of nematicity are considered. Our results suggest that in order to comprehensively understand this unique family of FeSe_{1-x}S_x, future theories should include the effects of nematicity and quantum paramagnetism, where multiple spin fluctuation-mediated pairing channels cooperate.

Acknowledgements: We gratefully acknowledge Moritz Hoesh, Pavel Dudin and Timur Kim for the experimental assistance at Diamond Light Source, and Yan Zhang for helpful discussions and sharing his unpublished data of independent measurement, and Jiangping Hu, Dung-Hai Lee, Andrey Chubukov, Rafael Fernandes, and Jian Kang for helpful discussions. This work is supported in part by the National Science Foundation of China, National Basic Research Program of China (973 Program) under the grant No. 2012CB921402, and the Science and Technology Committee of Shanghai under the grant No. 15YF1401000 and 15ZR1402900.

^{*} Electronic address: pengrui@fudan.edu.cn

[†] Electronic address: dlfeng@fudan.edu.cn

- P. J. Hirschfeld, M. M. Korshunov, and I. I. Mazin, Rep. Prog. Phys. 74, 124508 (2011).
- [2] J. K. Glasbrenner, I. I. Mazin, Harald O. Jeschke, P. J. Hirschfeld, R. M. Fernandes and Roser Valent? Nature Physics 11, 953-958 (2015).
- [3] R. Yu and Q. Si, Phys. Rev. Lett. 115, 116401 (2015).
- [4] Fa Wang, Steven A. Kivelson and Dung-Hai Lee, Nature Physics 11, 959-963 (2015).
- [5] H. Kontani, and S. Onari, Physical Review Letters 104, 157001 (2010).
- [6] Y. Zhang et al., Nat. Mater. 10, 273 (2011).
- [7] D. F. Liu et al., Nat. Commun. 3, 931 (2012).
- [8] M. Xu et al., Phys. Rev. B 85, 220504(R) (2012).
- [9] B. Zeng, B. Shen, G. F. Chen, J. B. He, D. M. Wang, C. H. Li, and H. H. Wen, Phys. Rev. B 83, 144511 (2011).
- [10] W. Yu, L. Ma, J. B. He, D. M. Wang, T. L. Xia, G. F. Chen, and W. Bao, Phys. Rev. Lett. 106, 197001 (2011).
- [11] J. T. Park et al., Phys. Rev. Lett. 107, 177005 (2011).
- [12] R. Peng et al., Phys. Rev. Lett. 112, 107001 (2011).
- [13] Q. Fan et al., Nature Physics 11, 946-952(2015).
- [14] M. D. Watson et al., Physical Review B 91, 155106 (2015).
- [15] Y. Zhang et al., Preprint: http://arxiv.org/abs/1503.01556.
- [16] T. M. McQueen, A. J. Williams, P. W. Stephens, J. Tao, Y. Zhu, V. Ksenofontov, F. Casper, C. Felser, and R. J. Cava, Phys. Rev. Lett. 103, 057002 (2009).
- [17] Q. Wang et al., Nat. Mater. 15(2): 159-163 (2016).
- [18] Q. Wang et al., Preprint: http://arxiv.org/abs/1511.02485.
- [19] J. Y. Lin, Y. S. Hsieh, D. A. Chareev, A. N. Vasiliev, Y. Parsons, and H. D. Yang, Phys. Rev. B 84, 220507(R)(2011).
- [20] D. Chareev, E. Osadchii, T. Kuzmichev, J. Y. Lin, S. Kuzmichev, O. Volkova, and A. Vasiliev, Cryst. Eng. Comm. 15, 1989 (2013).
- [21] J. K. Dong, T. Y. Guan, S. Y. Zhou, X. Qiu, L. Ding, C. Zhang,

- U. Patel, Z. L. Xiao, and S. Y. Li, Phys. Rev. B **80**, 024518 (2009)
- [22] C. L. Song et al., Science 332, 1410-1413 (2011).
- [23] S. A. Moore, J. L. Curtis, C. Di Giorgio, E. Lechner, M. Abdel-Hafiez, O. S. Volkova, A. N. Vasiliev, D. A. Chareev, G. Karapetrov, and M. Iavarone Physical Review B 92, 235113(2015).
- [24] S. Kasahara et al., Proc Natl Acad Sci U S A 111, 16309-16313.(2014).
- [25] M. Abdel-Hafiez et al., Physical Review B 91, 165109 (2015).
- [26] D. Chareev, E. Osadchii, T. Kuzmichev, J. Y. Lin, S. Kuzmichev, O. Volkova, and A. Vasiliev, Cryst. Eng. Commun. 15, 1989 (2013).
- [27] M. D. Watson, T. K. Kim, A. A. Haghighirad, S. F. Blake, N. R. Davies, M. Hoesch, T. Wolf, and A. I. Coldea, Phys. Rev. B 92, 121108 (2015).
- [28] J. Maletz et al., Phys. Rev. B 89, 220506 (2014).
- [29] See Supplementary Material at (link) for information on the superconducting gap distribution on pocket α along k_z .
- [30] Y. Zhang, Z. R. Ye, Q. Q. Ge, F. Chen, Juan Jiang, M. Xu, B. P. Xie and D. L. Feng, Nat. Phys. 8, 371-375 (2012).
- [31] Y. Zhang et al., Phys. Rev. Lett. 105, 117003 (2010).
- [32] D. J. Scalapino, Reviews of Modern Physics 84, 1383-1417 (2012).
- [33] J. Hu, and H. Ding, Sci Rep 2, 381 (2012).
- [34] S. Maiti, R. M. Fernandes, and A. V. Chubukov, Phys. Rev. B 85, 144527 (2012).
- [35] Z. P. Yin, K. Haule and G. Kotliar, Nature Physics 10, 845-850 (2014).
- [36] X. Lu, C. Fang, W. F. Tsai, Y. Jiang, and J. Hu, Phys. Rev. B 85, 054505 (2012).
- [37] Jian Kang, Alexander F. Kemper, Rafael M. Fernandes, Physical Review Letters **113**(21): 217001 (2014).